ELSEVIER

Search for single-top production in *ep* collisions at HERA

ZEUS Collaboration

S. Chekanov, M. Derrick, D. Krakauer, J.H. Loizides[1], S. Magill, B. Musgrave,
J. Repond, R. Yoshida

Argonne National Laboratory, Argonne, IL 60439-4815, USA[43]

M.C.K. Mattingly

Andrews University, Berrien Springs, MI 49104-0380, USA

P. Antonioli, G. Bari, M. Basile, L. Bellagamba, D. Boscherini, A. Bruni, G. Bruni,
G. Cara Romeo, L. Cifarelli, F. Cindolo, A. Contin, M. Corradi, S. De Pasquale,
P. Giusti, G. Iacobucci, A. Margotti, R. Nania, F. Palmonari, A. Pesci, G. Sartorelli,
A. Zichichi

University and INFN Bologna, Bologna, Italy[34]

G. Aghuzumtsyan, D. Bartsch, I. Brock, S. Goers, H. Hartmann, E. Hilger, P. Irrgang,
H.-P. Jakob, A. Kappes[2], U.F. Katz[2], O. Kind, U. Meyer, E. Paul[3], J. Rautenberg,
R. Renner, A. Stifutkin, J. Tandler, K.C. Voss, M. Wang, A. Weber[4]

Physikalisches Institut der Universität Bonn, Bonn, Germany[31]

D.S. Bailey[5], N.H. Brook[5], J.E. Cole, B. Foster, G.P. Heath, H.F. Heath, S. Robins,
E. Rodrigues[6], J. Scott, R.J. Tapper, M. Wing

H.H. Wills Physics Laboratory, University of Bristol, Bristol, United Kingdom[42]

M. Capua, A. Mastroberardino, M. Schioppa, G. Susinno

Calabria University, Physics Department and INFN, Cosenza, Italy[34]

J.Y. Kim, Y.K. Kim, J.H. Lee, I.T. Lim, M.Y. Pac[7]

Chonnam National University, Kwangju, South Korea[36]

A. Caldwell [8], M. Helbich, X. Liu, B. Mellado, Y. Ning, S. Paganis, Z. Ren,
W.B. Schmidke, F. Sciulli

Nevis Laboratories, Columbia University, Irvington on Hudson, NY 10027, USA [44]

J. Chwastowski, A. Eskreys, J. Figiel, K. Olkiewicz, P. Stopa, L. Zawiejski

Institute of Nuclear Physics, Cracow, Poland [38]

L. Adamczyk, T. Bołd, I. Grabowska-Bołd, D. Kisielewska, A.M. Kowal, M. Kowal,
T. Kowalski, M. Przybycień, L. Suszycki, D. Szuba, J. Szuba [9]

Faculty of Physics and Nuclear Techniques, University of Mining and Metallurgy, Cracow, Poland [45]

A. Kotański [10], W. Słomiński [11]

Department of Physics, Jagellonian University, Cracow, Poland

L.A.T. Bauerdick [12], U. Behrens, I. Bloch, K. Borras, V. Chiochia, D. Dannheim,
G. Drews, J. Fourletova, U. Fricke, A. Geiser, F. Goebel [8], P. Göttlicher [13], O. Gutsche,
T. Haas, W. Hain, G.F. Hartner, S. Hillert, B. Kahle, U. Kötz, H. Kowalski [14],
G. Kramberger, H. Labes, D. Lelas, B. Löhr, R. Mankel, I.-A. Melzer-Pellmann,
M. Moritz [15], C.N. Nguyen, D. Notz, M.C. Petrucci [16], A. Polini,
A. Raval, U. Schneekloth, F. Selonke [3], H. Wessoleck, G. Wolf,
C. Youngman, W. Zeuner

Deutsches Elektronen-Synchrotron DESY, Hamburg, Germany

S. Schlenstedt

DESY Zeuthen, Zeuthen, Germany

G. Barbagli, E. Gallo, C. Genta, G. Pelfer

University and INFN, Florence, Italy [34]

A. Bamberger, A. Benen

Fakultät für Physik der Universität Freiburg i.Br., Freiburg i.Br., Germany [31]

M. Bell, P.J. Bussey, A.T. Doyle, C. Glasman, J. Hamilton, S. Hanlon, S.W. Lee,
A. Lupi, D.H. Saxon, I.O. Skillicorn

Department of Physics and Astronomy, University of Glasgow, Glasgow, United Kingdom [42]

I. Gialas

Department of Engineering in Management and Finance, University of Aegean, Greece

B. Bodmann, T. Carli, U. Holm, K. Klimek, N. Krumnack, E. Lohrmann, M. Milite,
H. Salehi, S. Stonjek [17], K. Wick, A. Ziegler, Ar. Ziegler

Hamburg University, Institute of Experimental Physics, Hamburg, Germany [31]

C. Collins-Tooth, C. Foudas, R. Gonçalo [6], K.R. Long, A.D. Tapper

Imperial College London, High Energy Nuclear Physics Group, London, United Kingdom [42]

P. Cloth, D. Filges

Forschungszentrum Jülich, Institut für Kernphysik, Jülich, Germany

M. Kuze, K. Nagano, K. Tokushuku [18], S. Yamada, Y. Yamazaki

Institute of Particle and Nuclear Studies, KEK, Tsukuba, Japan [35]

A.N. Barakbaev, E.G. Boos, N.S. Pokrovskiy, B.O. Zhautykov

Institute of Physics and Technology of Ministry of Education and Science of Kazakhstan, Almaty, Kazakhstan

H. Lim, D. Son

Kyungpook National University, Taegu, South Korea [36]

K. Piotrzkowski

Institut de Physique Nucléaire, Université Catholique de Louvain, Louvain-la-Neuve, Belgium

F. Barreiro, O. González, L. Labarga, J. del Peso, E. Tassi, J. Terrón, M. Vázquez

Departamento de Física Teórica, Universidad Autónoma de Madrid, Madrid, Spain [41]

M. Barbi, F. Corriveau, S. Gliga, J. Lainesse, S. Padhi, D.G. Stairs

Department of Physics, McGill University, Montréal, PQ, Canada H3A 2T8 [30]

T. Tsurugai

Meiji Gakuin University, Faculty of General Education, Yokohama, Japan

A. Antonov, P. Danilov, B.A. Dolgoshein, D. Gladkov, V. Sosnovtsev, S. Suchkov

Moscow Engineering Physics Institute, Moscow, Russia [39]

R.K. Dementiev, P.F. Ermolov, Yu.A. Golubkov, I.I. Katkov, L.A. Khein,
I.A. Korzhavina, V.A. Kuzmin, B.B. Levchenko [19], O.Yu. Lukina, A.S. Proskuryakov,
L.M. Shcheglova, N.N. Vlasov, S.A. Zotkin

Moscow State University, Institute of Nuclear Physics, Moscow, Russia [40]

N. Coppola, S. Grijpink, E. Koffeman, P. Kooijman, E. Maddox, A. Pellegrino, S. Schagen, H. Tiecke, J.J. Velthuis, L. Wiggers, E. de Wolf

NIKHEF and University of Amsterdam, Amsterdam, Netherlands [37]

N. Brümmer, B. Bylsma, L.S. Durkin, T.Y. Ling

Physics Department, Ohio State University, Columbus, OH 43210, USA [43]

S. Boogert, A.M. Cooper-Sarkar, R.C.E. Devenish, J. Ferrando, G. Grzelak, T. Matsushita, S. Patel, M. Rigby, M.R. Sutton, R. Walczak

Department of Physics, University of Oxford, Oxford, United Kingdom [42]

A. Bertolin, R. Brugnera, R. Carlin, F. Dal Corso, S. Dusini, A. Garfagnini, S. Limentani, A. Longhin, A. Parenti, M. Posocco, L. Stanco, M. Turcato

Dipartimento di Fisica dell' Università and INFN, Padova, Italy [34]

E.A. Heaphy, F. Metlica, B.Y. Oh, P.R.B. Saull [20], J.J. Whitmore [21]

Department of Physics, Pennsylvania State University, University Park, PA 16802, USA [44]

Y. Iga

Polytechnic University, Sagamihara, Japan [35]

G. D'Agostini, G. Marini, A. Nigro

Dipartimento di Fisica, Università 'La Sapienza' and INFN, Rome, Italy [34]

C. Cormack [22], J.C. Hart, N.A. McCubbin

Rutherford Appleton Laboratory, Chilton, Didcot, Oxon, United Kingdom [42]

C. Heusch

University of California, Santa Cruz, CA 95064, USA [43]

I.H. Park

Department of Physics, Ewha Womans University, Seoul, South Korea

N. Pavel

Fachbereich Physik der Universität-Gesamthochschule Siegen, Germany

H. Abramowicz, A. Gabareen, S. Kananov, A. Kreisel, A. Levy

Raymond and Beverly Sackler Faculty of Exact Sciences, School of Physics, Tel Aviv University, Tel Aviv, Israel [33]

T. Abe, T. Fusayasu, S. Kagawa, T. Kohno, T. Tawara, T. Yamashita

Department of Physics, University of Tokyo, Tokyo, Japan [35]

R. Hamatsu, T. Hirose [3], M. Inuzuka, S. Kitamura [23], K. Matsuzawa, T. Nishimura

Tokyo Metropolitan University, Department of Physics, Tokyo, Japan [35]

M. Arneodo [24], M.I. Ferrero, V. Monaco, M. Ruspa, R. Sacchi, A. Solano

Università di Torino, Dipartimento di Fisica Sperimentale and INFN, Torino, Italy [34]

T. Koop, G.M. Levman, J.F. Martin, A. Mirea

Department of Physics, University of Toronto, Toronto, ON, Canada M5S 1A7 [30]

J.M. Butterworth, C. Gwenlan, R. Hall-Wilton, T.W. Jones, M.S. Lightwood, B.J. West

Physics and Astronomy Department, University College London, London, United Kingdom [42]

J. Ciborowski [25], R. Ciesielski [26], R.J. Nowak, J.M. Pawlak, J. Sztuk [27],
T. Tymieniecka [28], A. Ukleja [28], J. Ukleja, A.F. Żarnecki

Warsaw University, Institute of Experimental Physics, Warsaw, Poland [46]

M. Adamus, P. Plucinski

Institute for Nuclear Studies, Warsaw, Poland [46]

Y. Eisenberg, L.K. Gladilin [29], D. Hochman, U. Karshon

Department of Particle Physics, Weizmann Institute, Rehovot, Israel [32]

D. Kçira, S. Lammers, L. Li, D.D. Reeder, A.A. Savin, W.H. Smith

Department of Physics, University of Wisconsin, Madison, WI 53706, USA [43]

A. Deshpande, S. Dhawan, V.W. Hughes, P.B. Straub

Department of Physics, Yale University, New Haven, CT 06520-8121, USA [43]

S. Bhadra, C.D. Catterall, S. Fourletov, S. Menary, M. Soares, J. Standage

Department of Physics, York University, ON, Canada M3J 1P3 [30]

Abstract

A search for single-top production, $ep \rightarrow etX$, has been made with the ZEUS detector at HERA using an integrated luminosity of 130.1 pb^{-1}. Events from both the leptonic and hadronic decay channels of the W boson resulting from the decay of the top quark were sought. For the leptonic mode, the search was made for events with isolated high-energy leptons and significant missing transverse momentum. For the hadronic decay mode, three-jet events in which two of the jets had an invariant mass consistent with that of the W were selected. No evidence for top production was found. The results are used to constrain single-top production via flavour-changing neutral current (FCNC) transitions. The ZEUS limit excludes a substantial region in the FCNC $tu\gamma$ coupling not ruled out by other experiments.

1. Introduction

The Standard Model (SM) of the fundamental interactions presently provides an accurate description of the phenomena observed in both low- and high-energy reactions of elementary particles. As probes in search for physics beyond the SM, observables sensitive to flavour-changing neutral current (FCNC) interactions are particularly useful, since the SM rates are very small due to the GIM mechanism [1]. The FCNC interactions involving the top quark [2,3], which has a mass of the order of the electroweak energy scale, offer a potentially new view of physics beyond the SM.

The FCNC-induced couplings of the type tuV or tcV (with $V = \gamma, Z^0$) have been explored in $p\bar{p}$ collisions at the Tevatron by searching for the top-quark decays $t \to uV$ and $t \to cV$ [4]. The same couplings involving the top quark were investigated in e^+e^- interactions at LEP2 by searching for single-top production through the reactions $e^+e^- \to t\bar{u}$ (+c.c.) and $e^+e^- \to t\bar{c}$ (+c.c.) [5,6]. No evidence for such interactions was found at either accelerator and limits were set on the branching ratios $B(t \to q\gamma)$ and $B(t \to qZ)$.

In ep collisions at the HERA collider, top quarks can only be singly produced. In the SM, single-top production proceeds through the charged current (CC) reaction $ep \to \nu t\bar{b}X$ [7]. Since the SM cross section at HERA is less than 1 fb [8], any observed single-top event in the present data can be attributed to physics beyond the SM. The FCNC couplings, tuV or tcV, would induce the neutral current (NC) reaction $ep \to etX$ [3,9], in which the incoming lepton exchanges a γ or Z with an up-type quark in the proton, yielding a top quark in the final state. Due to the large Z mass, this process is most sensitive to a coupling of the type $tq\gamma$. Furthermore, large values of x, the fraction of the proton momentum carried by the struck quark, are needed to produce a top. Since the u-quark parton distribution function (PDF) of the proton is dominant at large x, the production of single top quarks is most sensitive to a coupling of the type $tu\gamma$ (see Fig. 1).

2. Theoretical framework

Deviations from the SM predictions due to FCNC transitions involving the top quark can be parame-
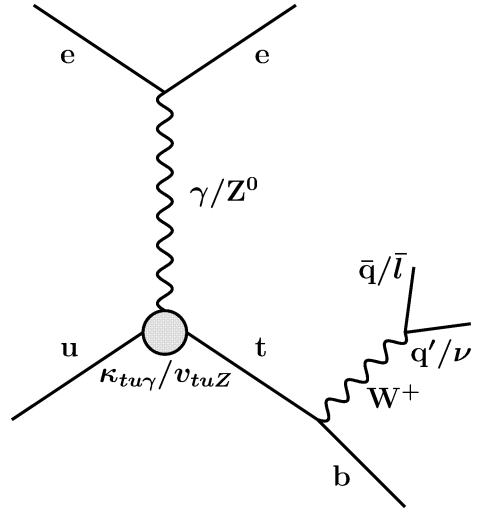
Fig. 1. Single-top production via flavour-changing neutral current transitions at HERA.

terised in terms of couplings of the type tuV (with $V = \gamma, Z^0$) and described by an effective Lagrangian of the form [10]

$$\Delta\mathcal{L}_{\text{eff}} = ee_t\bar{t}\frac{i\sigma_{\mu\nu}q^\nu}{\Lambda}\kappa_{tu\gamma}uA^\mu$$
$$+ \frac{g}{2\cos\theta_W}\bar{t}\gamma_\mu v_{tuZ}uZ^\mu + \text{h.c.}, \qquad (1)$$

where e (e_t) is the electron (top-quark) electric charge, g is the weak coupling constant, θ_W is the weak mixing angle, $\sigma_{\mu\nu} = \frac{1}{2}(\gamma^\mu\gamma^\nu - \gamma^\nu\gamma^\mu)$, Λ is an effective cutoff which, by convention, is set to the mass of the top quark, M_{top}, taken as 175 GeV, q is the momentum of the gauge boson and A^μ (Z^μ) is the photon (Z) field. In the following, it was assumed that the magnetic coupling $\kappa_{tu\gamma}$ and the vector coupling v_{tuZ} are real and positive. The values of $\kappa_{tu\gamma}$ and v_{tuZ} in the SM are zero at tree level and extremely small at the one-loop level.

The cross section for the process $ep \to etX$ was calculated as a function of $\kappa_{tu\gamma}$ including next-to-leading-order (NLO) QCD corrections in the eikonal approximation [9]. The renormalisation (μ_R) and factorisation (μ_F) scales were chosen to be $\mu_R = \mu_F = M_{\text{top}}$. The strong coupling constant, α_s, was calculated at two loops with $\Lambda_{\overline{\text{MS}}}^{(5)} = 220$ MeV, corresponding to $\alpha_s(M_Z) = 0.1175$. The calculations were performed using the MRST99 [11] parameterisations of the proton PDFs. The uncertainty of the results due to terms

beyond NLO, estimated by varying $\mu_R = \mu_F$ between $M_{\text{top}}/2$ and $2M_{\text{top}}$, was $^{+1.6}_{-3.8}\%$ $(^{+1.3}_{-3.6}\%)$ at a centre-of-mass energy of 318 (300) GeV. The uncertainties of the results due to that on $\alpha_s(M_Z)$ and on the proton PDFs were $\pm 2\%$ and $\pm 4\%$, respectively. The variation of the cross section on M_{top} was approximately $\pm 20\%$ ($\pm 25\%$) for $\Delta M_{\text{top}} = \pm 5$ GeV at a centre-of-mass energy of 318 (300) GeV.

3. Experimental conditions

The data samples were collected with the ZEUS detector at HERA and correspond to an integrated luminosity of $47.9 \pm 0.9(65.5 \pm 1.5)$ pb^{-1} for $e^+ p$ collisions taken during 1994–1997 (1999–2000) and 16.7 ± 0.3 pb^{-1} for $e^- p$ collisions taken during 1998–1999. During 1994–1997 (1998–2000), HERA operated with protons of energy $E_p = 820$ GeV (920 GeV) and positrons or electrons of energy $E_e = 27.5$ GeV, yielding a centre-of-mass energy of $\sqrt{s} = 300$ GeV (318 GeV).

The ZEUS detector is described in detail elsewhere [12,13]. The main components used in the present analysis were the central tracking detector (CTD) [14], positioned in a 1.43 T solenoidal magnetic field, and the uranium-scintillator sampling calorimeter (CAL) [15].

Tracking information is provided by the CTD, in which the momenta of tracks in the polar-angle[47] region $15° < \theta < 164°$ are reconstructed. The CTD consists of 72 cylindrical drift chamber layers, organised in nine superlayers. The relative transverse momentum, p_T, resolution for full-length tracks can be parameterised as $\sigma(p_T)/p_T = 0.0058 p_T \oplus 0.0065 \oplus 0.0014/p_T$, with p_T in GeV.

The CAL covers 99.7% of the total solid angle. It is divided into three parts with a corresponding division in θ, as viewed from the nominal interaction point: forward (FCAL, $2.6° < \theta < 36.7°$), barrel (BCAL, $36.7° < \theta < 129.1°$), and rear (RCAL, $129.1° < \theta < 176.2°$). Each of the CAL parts is subdivided into

towers which in turn are segmented longitudinally into one electromagnetic (EMC) and one (RCAL) or two (FCAL, BCAL) hadronic (HAC) sections. The smallest subdivision of the CAL is called a cell. Under test-beam conditions, the CAL single-particle energy resolution is $\sigma(E)/E = 18\%/\sqrt{E}$ for electrons and $\sigma(E)/E = 35\%/\sqrt{E}$ for hadrons, with E in GeV.

The luminosity was measured using the Bethe–Heitler reaction $ep \to e\gamma p$. The resulting small-angle energetic photons were measured by the luminosity monitor [16], a lead-scintillator calorimeter placed in the HERA tunnel at $Z = -107$ m.

3.1. Trigger conditions

A three-level trigger was used to select events online [12,17]. At the first level, events were selected using criteria based on either the transverse energy or missing transverse momentum measured in the CAL. Events were accepted with a low threshold on these quantities when a coincidence with CTD tracks from the event vertex was required, while a higher threshold was used for events with no CTD tracks.

At the second level, timing information from the CAL was used to reject events inconsistent with an ep interaction. In addition, the topology of the CAL energy deposits was used to reject non-ep background events. Cuts on the missing transverse momentum of 6 GeV (9 GeV for events without CTD tracks) or on the total transverse energy of 8 GeV, excluding the eight CAL towers immediately surrounding the forward beampipe, were applied.

At the third level, track reconstruction and vertex finding were performed and used to reject events with a vertex inconsistent with the distribution of ep interactions. Events with missing transverse momentum in excess of 7 GeV or containing at least two jets with transverse energy $E_T^{\text{jet}} > 6$ GeV and pseudorapidity $\eta^{\text{jet}} < 2.5$ were accepted; the latter condition was based upon the application of a jet-finding cone algorithm with radius $R = 1$ applied to the CAL cell energies and positions.

4. Monte Carlo simulation

Samples of events were generated using Monte Carlo (MC) simulations to determine the selection

---

[47] The ZEUS coordinate system is a right-handed Cartesian system, with the Z-axis pointing in the proton beam direction, referred to as the "forward direction", and the X-axis pointing left towards the centre of HERA. The coordinate origin is at the nominal interaction point.

efficiency for the signal of single-top production through FCNC processes and to estimate background rates from SM processes. The generated events were passed through the GEANT 3.13-based [18] ZEUS detector- and trigger-simulation programs [12]. They were reconstructed and analysed by the same program chain as the data.

Single-top production through FCNC processes in ep collisions was simulated using the HEXF generator [19]. Samples of events were generated assuming top-quark masses of 170, 175 and 180 GeV. Initial-state radiation from the lepton beam was included using the Weizsäcker–Williams approximation [20]. The hadronic final state was simulated using the matrix-element and parton-shower model of LEPTO [21] for the QCD cascade and the Lund string model [22] as implemented in JETSET [23] for the hadronisation. The MRSA [24] parameterisations of the proton PDFs were used.

The most important background to the positron-decay channel of the W in the chain $t \rightarrow bW^+ \rightarrow be^+\nu$ arose from NC deep inelastic scattering (DIS). Two-photon processes provide a source of high-p_T leptons that were a significant background to the muon-decay channel of the W in the chain $t \rightarrow bW^+ \rightarrow b\mu^+\nu$. In addition, single-$W$ production was a significant source of background to $t \rightarrow bW^+$, in both the positron- and muon-decay channels of the W. The dominant source of background for the hadronic-decay channel of W in the chain $t \rightarrow bW^+ \rightarrow bq\bar{q}'$ was multi-jet production from QCD processes.

Several MC programs were used to simulate the different background processes. The NC DIS events were generated using the LEPTO 6.5 program [21] interfaced to HERACLES 4.6.1 [25] via DJANGOH 1.1 [26]. The HERACLES program includes photon and Z exchanges and first-order electroweak radiative corrections. The QCD cascade was modelled with the colour-dipole model [27] by using the ARIADNE 4.08 program [28] and including the boson–gluon-fusion process. As an alternative, samples of events were generated using the model of LEPTO based on first-order QCD matrix elements plus parton showers (MEPS). In both cases, the hadronisation was performed using the Lund string model. The CTEQ5D [29] parameterisations for the proton PDFs were used. Two-photon processes were simulated using the generator GRAPE 1.1 [30], which includes dilepton production

via $\gamma\gamma$, $Z\gamma$ and ZZ processes and considers both elastic and inelastic production at the proton vertex. Single-W production was simulated using the event generator EPVEC [31], which did not include hard QCD radiation. Recent cross-section calculations including higher-order QCD corrections [32] and using the CTEQ4M [33] (ACFGP [34]) proton (photon) PDFs were used to reweight the EPVEC event samples. Multi-jet QCD production at low Q^2, where Q^2 is the virtuality of the exchanged photon, was simulated using PYTHIA 5.7 [35]. In this generator, the partonic processes were simulated using leading-order (LO) matrix elements, with the inclusion of initial- and final-state parton showers. Hadronisation was performed using the Lund string model. The MRSA (GRV-HO [36]) parameterisations of the proton (photon) PDFs were used.

5. Signatures of FCNC-induced single-top production

Single-top production via the FCNC coupling at the $tu\gamma$ vertex in ep collisions at HERA, $ep \rightarrow etX$, is predicted to proceed predominantly through the exchange of a quasi-real photon between the beam electron or positron and a valence u quark in the proton (see Fig. 1). According to the signal MC simulation, the scattered electron or positron escapes through the rear beampipe, outside the CAL acceptance, in 65% of the events.

In this analysis, the top-quark search was optimised for the decay $t \rightarrow bW^+$. In the leptonic decay channel of the W, the signal for such events is the presence of an isolated high-energy lepton, significant missing transverse momentum arising from the emitted neutrino and a jet stemming from the b-quark decay. In the hadronic decay channel of the W, the signal is the presence of three jets in the final state with the di-jet invariant-mass distribution for the correct pair of jets peaking at the mass of the W boson, M_W, and the three-jet invariant-mass distribution peaking at M_{top}.

6. Leptonic channel

6.1. Data selection

Events with isolated high-energy leptons ($e^\pm$ or $\mu^\pm$), significant missing transverse momentum and a

jet were selected. Similar previous analyses have been done by the H1 [37] and ZEUS [38] Collaborations. Positron candidates were identified using an algorithm that combined CAL and CTD information [39]. Muons were identified by the coincidence of a track in the CTD with significant transverse momentum and CAL energy deposits consistent with those expected from a minimum ionizing particle. The charge information on the candidates was not used and they are generically referred to as positrons and muons. The main selection criteria are:

- cuts on the CAL timing and Z coordinate ($|Z| < 50$ cm) of the event vertex and algorithms based on the pattern of tracks in the CTD were used to reject events not originating from ep collisions;
- the track associated with the positron or muon candidate was required to have $p_T^{track} > 5$ GeV. To reduce the NC DIS background, the track was required to have $\theta < 115°$. In addition, it must have passed through at least three radial superlayers of the CTD (corresponding to $\theta \gtrsim 17°$) and be isolated. Two isolation variables were defined for a given track using the separation R in the η–ϕ plane, where $R = \sqrt{(\Delta\eta)^2 + (\Delta\varphi)^2}$. The variable D_{jet} was defined as the distance from the nearest jet axis, while D_{track} was the distance from the nearest neighbouring track in the event. Events containing tracks with $D_{jet} > 1$ and $D_{track} > 0.5$ were selected;
- $p_T^{CAL} > 20$ GeV, where p_T^{CAL} is the missing transverse momentum as measured with the CAL. It was reconstructed using the energy deposited in the CAL cells, after corrections for non-uniformity and dead material located in front of the CAL [40]. Energy deposits originating from identified muons were excluded from the measurement of p_T^{CAL};
- the presence of at least one jet with transverse energy E_T^{jet} above 5 GeV and $-1 < \eta^{jet} < 2.5$ was required. The longitudinally invariant k_T cluster algorithm [41] was used in the inclusive mode [42] to reconstruct jets from the energy deposits in the CAL cells. The jet search was performed in the η–ϕ plane of the laboratory frame. The axis of each jet was defined according to the Snowmass convention [43], where η^{jet} (φ^{jet}) was the transverse-energy-weighted mean pseudora-

pidity (azimuth) of all the cells belonging to that jet. The jet transverse energy was reconstructed as the sum of the transverse energies of the cells belonging to the jet and was corrected for detector effects such as energy losses in the inactive material in front of the CAL [44]. In the leptonic channel, only those jets for which the electromagnetic-energy fraction was below 0.9 and $R_{90\%} \geqslant 0.1$, where $R_{90\%}$ is the radius of the cone in the η–ϕ plane concentric to the jet axis that contains 90% of the jet energy, were considered;

- in events with an identified positron candidate, the acoplanarity angle, Φ_{ACOP}, was defined as the azimuthal separation of the outgoing positron and the vector in the (X, Y)-plane that balances the hadronic system. For well measured NC DIS events, the acoplanarity angle is close to zero, while a large Φ_{ACOP} indicates large missing energy, as expected from top-quark decays. To reduce the background from NC DIS processes, the acoplanarity angle was required to be greater than $8°$.

The selected data sample contained 36 events, 24 of which had a positron candidate and 12 a muon candidate (see Table 1).

6.2. Comparison with Monte Carlo simulations

The properties of the selected events were studied in detail and compared with the MC predictions of the SM. Fig. 2(a)–(c) show the acoplanarity, the transverse momentum of the hadronic system, p_T^{had}, and the transverse momentum of the positron candidate as measured in the CAL, p_T^e, for those events with an identified positron candidate. Fig. 2(d)–(f) show the CAL transverse momentum corrected for the muon momentum measured by the CTD, $p_T^{tot} = \sqrt{(p_X^{CAL} + p_X^\mu)^2 + (p_Y^{CAL} + p_Y^\mu)^2}$, p_T^{had} and the transverse momentum of the track associated with the muon candidate, p_T^μ, for events with an identified muon candidate. In each case, the distribution of data events can be accounted for by the simulation of SM processes. The SM expectation for the positron channel is dominated by NC DIS and that for the muon channel by two-photon processes.

Table 1

Number of events in data and Standard Model background for the leptonic channel for different samples after the preselection and final selection cuts. The percentage of single-W production included in the expectation is indicated in parentheses. The statistical and systematic uncertainties added in quadrature are also indicated

Leptonic channel	Positron channel obs./expected (W)	Muon channel obs./expected (W)
Preselection		
$e^+ p$, $\sqrt{s} = 300$ GeV $\left(\mathcal{L} = 47.9 \text{ pb}^{-1}\right)$	$4/7.3^{+0.8}_{-2.1}$	$0/4.2^{+0.4}_{-0.3}$
$e^- p$, $\sqrt{s} = 318$ GeV $\left(\mathcal{L} = 16.7 \text{ pb}^{-1}\right)$	$7/3.2^{+0.6}_{-1.0}$	$1/2.1^{+0.2}_{-0.2}$
$e^+ p$, $\sqrt{s} = 318$ GeV $\left(\mathcal{L} = 65.5 \text{ pb}^{-1}\right)$	$13/10.1^{+0.9}_{-1.9}$	$11/5.6^{+0.4}_{-0.4}$
Total $\left(\mathcal{L} = 130.1 \text{ pb}^{-1}\right)$	$24/20.6^{+1.7}_{-4.6}$ (17%)	$12/11.9^{+0.6}_{-0.7}$ (16%)
Final selection $\left(p_T^{\text{had}} > 25 \text{ GeV}\right)$		
$e^+ p$, $\sqrt{s} = 300$ GeV $\left(\mathcal{L} = 47.9 \text{ pb}^{-1}\right)$	$0/0.72^{+0.27}_{-0.13}$	$0/0.78^{+0.10}_{-0.10}$
$e^- p$, $\sqrt{s} = 318$ GeV $\left(\mathcal{L} = 16.7 \text{ pb}^{-1}\right)$	$1/0.64^{+0.28}_{-0.20}$	$1/0.45^{+0.07}_{-0.07}$
$e^+ p$, $\sqrt{s} = 318$ GeV $\left(\mathcal{L} = 65.5 \text{ pb}^{-1}\right)$	$1/1.54^{+0.33}_{-0.32}$	$4/1.53^{+0.17}_{-0.16}$
Total $\left(\mathcal{L} = 130.1 \text{ pb}^{-1}\right)$	$2/2.90^{+0.59}_{-0.32}$ (45%)	$5/2.75^{+0.21}_{-0.21}$ (50%)
Final selection $\left(p_T^{\text{had}} > 40 \text{ GeV}\right)$		
$e^+ p$, $\sqrt{s} = 300$ GeV $\left(\mathcal{L} = 47.9 \text{ pb}^{-1}\right)$	$0/0.23^{+0.05}_{-0.05}$	$0/0.26^{+0.04}_{-0.04}$
$e^- p$, $\sqrt{s} = 318$ GeV $\left(\mathcal{L} = 16.7 \text{ pb}^{-1}\right)$	$0/0.16^{+0.06}_{-0.06}$	$0/0.08^{+0.05}_{-0.01}$
$e^+ p$, $\sqrt{s} = 318$ GeV $\left(\mathcal{L} = 65.5 \text{ pb}^{-1}\right)$	$0/0.54^{+0.07}_{-0.07}$	$0/0.61^{+0.10}_{-0.09}$
Total $\left(\mathcal{L} = 130.1 \text{ pb}^{-1}\right)$	$0/0.94^{+0.11}_{-0.10}$ (61%)	$0/0.95^{+0.14}_{-0.10}$ (61%)

6.3. Results of the search in the leptonic channel

The final event selection for the $bl\nu$ final state required a high-p_T jet and missing energy. The cuts were optimised using the simulations of both the SM background and the expected single-top signal. The cuts used were:

- $p_T^{\text{had}} > 40$ GeV for both the positron and muon decays;
- $\delta = \sum_i (E_i - E_i \cos\theta_i) = \sum_i (E - p_Z)_i < 47$ GeV for the positron decay, where the sum runs over all CAL energy deposits with corrected energy E_i and polar angle θ_i [40]. For fully contained NC DIS events, δ peaks at 55 GeV, i.e., twice the lepton beam energy, which follows from energy–momentum conservation;
- $p_T^{\text{tot}} > 10$ GeV for the muon decay.

After applying these requirements, no event remained in the data sample. The efficiency for detecting single-top production in the leptonic channel was 34% for the positron decay and 33% for the muon decay.

These efficiencies do not include the branching ratio of the top-quark decay in the corresponding channel.

In a recent study [45], the H1 Collaboration has reported an excess of events for $p_T^{\text{had}} > 25$ GeV. The number of selected events in each channel with $p_T^{\text{had}} > 25$ GeV for the present analysis is also listed in Table 1. These results are in agreement with the expectations from the SM.

7. Hadronic channel

The data used for this channel correspond to a slightly reduced luminosity of 127.2 pb^{-1}.

7.1. Data selection

The expected signature for the hadronic-decay channel of single-top production through the FCNC $tu\gamma$ coupling is three jets with large E_T^{jet} and no significant missing transverse momentum. Since it is expected that for the bulk of the events the scattered
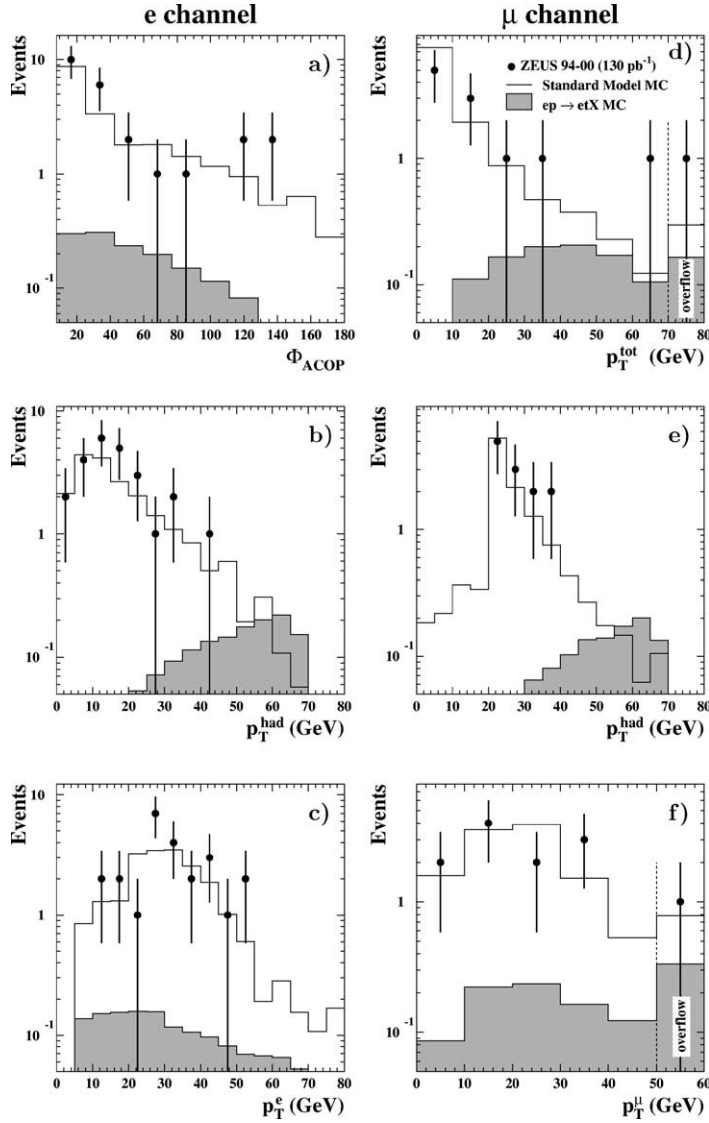
Fig. 2. (a) Φ_{ACOP}, (b) p_T^{had} and (c) p_T^e for those events with an identified positron candidate. (d) p_T^{tot}, (e) p_T^{had} and (f) p_T^μ for those events with an identified muon candidate. The dots are the data, the solid histogram is the Standard Model MC simulation and the shaded histogram represents the signal with $M_{\text{top}} = 175$ GeV normalised to the limit presented in Section 9. The final bins in (d) and (f), marked "overflow", contain all events above the lower boundaries of these bins. The distributions are for the selected events according to the criteria of Section 6.1. The Standard Model MC distributions have been normalised to the luminosity of the data.

positron escapes through the rear beam pipe, NC DIS events with $Q^2 \gtrsim 1$ GeV^2 were rejected. The data selection used similar criteria as reported in a previous publication [44]. Jets were found in the hadronic final state using the same algorithm as described in Section 6.1. The main selection criteria are:

• cuts on the Z coordinate ($-38 < Z < 32$ cm) of the event vertex, the number of tracks pointing to the vertex and the number of tracks compatible with an interaction upstream in the direction of the proton beam were used to reject events not originating from ep collisions;

- the presence of at least three jets within the pseudorapidity range $-1 < \eta^{\mathrm{jet}} < 2.5$ was required. The three highest-E_T^{jet} jets in the event, ordered according to decreasing E_T^{jet}, were further required to satisfy $E_T^{\mathrm{jet}(1,2,3)} > 40, 25, 14$ GeV;
- CC DIS events were rejected by requiring the missing transverse momentum to be small compared to the total transverse energy, E_T^{tot}, i.e., $p_T^{\mathrm{CAL}}/\sqrt{E_T^{\mathrm{tot}}} < 2\sqrt{\mathrm{GeV}}$;
- NC DIS events with an identified scattered-positron candidate [46] in the CAL were removed from the sample using the method described in an earlier publication [47];
- $8.8 < \delta < 52.2$ GeV. The upper cut removed unidentified NC DIS events and the lower cut rejected proton beam–gas interactions.

The selected sample contained 348 events.

The invariant mass of jets k and l was determined using the corrected jet transverse energies, as explained in Section 6.1, and jet angular variables according to the formula

$$M^{\mathrm{jj}} = \left\{ 2E_T^{\mathrm{jet},k} E_T^{\mathrm{jet},l} \left[\cosh\left(\eta^{\mathrm{jet},k} - \eta^{\mathrm{jet},l}\right) \right. \right.$$
$$\left. \left. - \cos\left(\varphi^{\mathrm{jet},k} - \varphi^{\mathrm{jet},l}\right) \right] \right\}^{1/2}.$$

The three-jet invariant mass, $M^{3\mathrm{j}}$, was reconstructed using the formula

$$M^{3\mathrm{j}} = \left\{ \sum_{k<l} 2E_T^{\mathrm{jet},k} E_T^{\mathrm{jet},l} \left[\cosh\left(\eta^{\mathrm{jet},k} - \eta^{\mathrm{jet},l}\right) \right. \right.$$
$$\left. \left. - \cos\left(\varphi^{\mathrm{jet},k} - \varphi^{\mathrm{jet},l}\right) \right] \right\}^{1/2},$$

where the sum runs over $k, l = 1, 2, 3$. The average resolution in M^{jj} was 8% for $M^{\mathrm{jj}} > 50$ GeV and the distribution of M^{jj} for all pairs of jets in a sample of MC signal events is shown in Fig. 3(a). The average resolution in $M^{3\mathrm{j}}$ was 4% for $M^{3\mathrm{j}} > 80$ GeV and the $M^{3\mathrm{j}}$ distribution in a sample of MC signal events is shown in Fig. 3(b). Cuts on M^{jj} and $M^{3\mathrm{j}}$ were used to search for a signal of single-top production in the hadronic channel.

7.2. Comparison with Monte Carlo simulations

The properties of the selected events were studied in detail and were compared with the MC predictions of the SM processes. The MC distributions were normalised to the number of events in the data with $M^{3\mathrm{j}} < 159$ GeV, i.e., outside the region where the signal for single-top production is expected. The resulting normalisation factor was 1.11 ± 0.08, which can be attributed to higher-order QCD corrections to the jet cross sections. The simulations of SM processes provide a reasonable description of the E_T^{jet} and η^{jet} data distributions (not shown). The distribution of M^{jj} for all pairs of jets in an event and that of $M^{3\mathrm{j}}$ are presented in Fig. 3(a) and (b), respectively. The $M^{3\mathrm{j}}$ distribution shows a steep fall-off from $M^{3\mathrm{j}} \sim 130$ to 240 GeV. The SM simulations describe the observed M^{jj} and $M^{3\mathrm{j}}$ distributions reasonably well.

7.3. Results of the search in the hadronic channel

The MC simulations of the signal and SM processes were used to find optimal windows in M^{jj} and $M^{3\mathrm{j}}$ for the observation of a signal relative to the background. The resulting windows were $65.2 < M^{\mathrm{jj}} < 90.8$ GeV and $159 < M^{3\mathrm{j}} < 188$ GeV.

The M^{jj} closest to M_W is denoted by M_W^{jj}. The distribution of M_W^{jj} is shown in Fig. 3(c); 261 events in the data satisfied the condition $65.2 < M_W^{\mathrm{jj}} < 90.8$ GeV. The $M^{3\mathrm{j}}$ distribution after this cut is shown in Fig. 3(d). The simulation of SM processes reproduces the distributions well. After the requirement $159 < M^{3\mathrm{j}} < 188$ GeV, 14 events remained. The distributions of M_W^{jj} and $M^{3\mathrm{j}}$ in the data after this cut are shown in Fig. 3(e) and (f), respectively, and are well reproduced by the simulation of SM processes. After these cuts, the efficiency for detecting single-top production in the hadronic channel was 24%. This efficiency does not include the branching ratio of the top-quark decay in the hadronic channel. The observed $M^{3\mathrm{j}}$ distribution shows no significant excess at M_{top}.

8. Systematic uncertainties

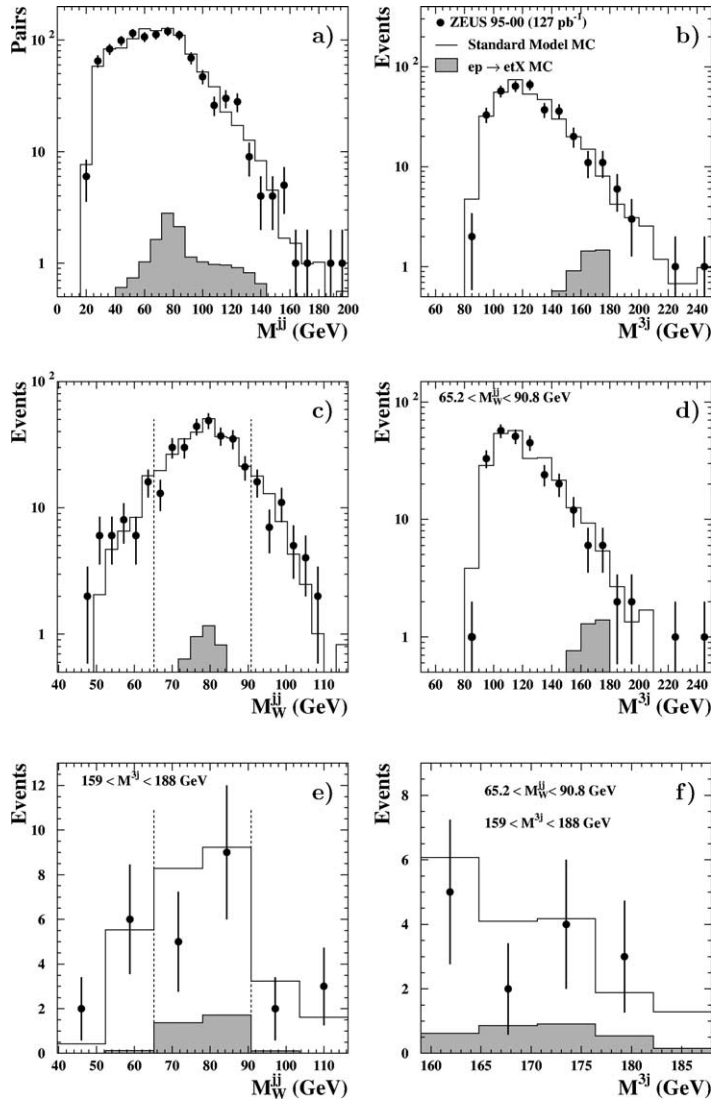The most important sources of systematic uncertainty were:

Fig. 3. (a) M^{ij} (for all pairs of jets), (b) M^{3j} and (c) M_W^{ij} distributions for the sample of events selected in the hadronic channel; (d) M^{3j} distribution for those events with $65.2 < M_W^{ij} < 90.8$ GeV; (e) M_W^{ij} distribution for those events with $159 < M^{3j} < 188$ GeV; (f) M^{3j} distribution for those events with $65.2 < M_W^{ij} < 90.8$ GeV. The dashed lines in (c) and (e) represent the cut at $65.2 < M_W^{ij} < 90.8$ GeV. The distributions are for three-jet events with $E_T^{jet1} > 40$, $E_T^{jet2} > 25$, $E_T^{jet3} > 14$ GeV and $-1 < \eta^{jet} < 2.5$. Other details are given in the caption to Fig. 2.

- leptonic channel
  − the uncertainty of $\pm 1\%$ on the absolute energy scale of the CAL gave changes of $^{+6.7}_{-1.6}\%$ in the background and negligible changes in the signal-efficiency estimations;
  − the use of the LEPTO-MEPS model instead of ARIADNE to estimate the NC DIS background

gave a change of -0.8% in the background estimation;
  − the MC statistical uncertainty on the SM background estimation was $\pm 7.5\%$;
- hadronic channel
  − the uncertainty of $\pm 1\%$ on the absolute energy scale of the jets [44] gave changes of $^{+10.4}_{-1.7}\%$ in

Table 2
Number of events in data and Standard Model background for the leptonic and hadronic channels for different samples, together with the efficiency times branching ratio of the signal and luminosity for each sample. The last four rows show the limits on the single-top production cross section via flavour-changing neutral current transitions and on the $\kappa_{tu\gamma}$ coupling assuming $M_{\text{top}} = 175$ GeV

		Leptonic channel		Hadronic channel	
	$\sqrt{s} =$	300 GeV	318 GeV	300 GeV	318 GeV
N_{obs}		0	0	5	9
N_{SM}		$0.49^{+0.07}_{-0.07}$	$1.40^{+0.17}_{-0.13}$	$3.3^{+1.3}_{-0.4}$	$14.3^{+1.2}_{-1.1}$
$\epsilon \cdot \text{Br}$ (%)		6.9	7.1	16.6	16.5
Luminosity (pb^{-1})		47.9	82.2	45.0	82.2
$\sigma_{\text{lim}} \times B(t \to Wb)$ (pb)		0.906	0.514	0.998	0.426
$\kappa_{tu\gamma}$ (per channel)			0.223		0.241
σ_{lim} (pb) (all channels)			0.225 at $\sqrt{s} = 318$ GeV		
$\kappa_{tu\gamma}$ (all channels)			0.174		

the background and $^{+3.9}_{-4.9}$% in the signal-efficiency estimations;

− the MC normalisation uncertainty on the SM background estimation was ± 7.4%.

All these uncertainties in the number of expected background events were added in quadrature and are shown in Tables 1 and 2. The experimental uncertainties were smaller than the theoretical uncertainties and, therefore, were not considered in the derivation of the limits for single-top production.

9. Limit on the FCNC couplings

As no event was selected in the leptonic channel and no excess over the SM prediction was observed in the hadronic channel (see Table 2), limits were set on FCNC couplings of the type tqV. The contribution of the charm quark, which has only a small density in the proton at high x, was ignored by setting $\kappa_{tc\gamma} = v_{tcZ} = 0$. Only the anomalous couplings involving a u quark, $\kappa_{tu\gamma}$ and v_{tuZ}, were considered.

At HERA, most of the sensitivity to FCNC-induced couplings involving the top quark comes from the process $ep \to etX$ in which a γ is exchanged since the large Z mass suppresses the contribution due to Z exchange. In a first step, limits on $\kappa_{tu\gamma}$ were, therefore, derived assuming $v_{tuZ} = 0$ and using NLO QCD calculations of the cross section for the process $ep \to etX$ (see Section 2). The results obtained from each channel and centre-of-mass energy together with

those from the combined analysis presented below are summarised in Table 2. Limits from a combination of channels were obtained by using a method described in a previous publication [48]. In the derivation of the limits, the decrease in the branching ratio $B(t \to Wb)$ in the presence of FCNC decays was taken into account. In comparison to the dependence of the result on the assumed value of M_{top}, the effects of all other uncertainties are very small. Therefore, limits were evaluated for $M_{\text{top}} = 170$, 175 and 180 GeV, neglecting the other uncertainties.

By combining the results from both the leptonic and hadronic channels, an upper limit of

$$\kappa_{tu\gamma} < 0.174 \text{ at } 95\% \text{ C.L.,}$$

was derived assuming $M_{\text{top}} = 175$ GeV. The limit was $\kappa_{tu\gamma} < 0.158 \ (0.210)$ for $M_{\text{top}} = 170(180)$ GeV. The above coupling limit corresponds to a limit on the cross section for single-top production of

$$\sigma\left(ep \to etX, \sqrt{s} = 318 \text{ GeV}\right)$$
$$< 0.225 \text{ pb at } 95\% \text{ C.L.}$$

In a second step, the effects of a non-zero v_{tuZ} coupling were taken into account. The derivation of the exclusion region in the $\kappa_{tu\gamma}$–v_{tuZ} plane was made using LO calculations for the process $ep \to etX$ obtained with the program CompHEP [49], since NLO corrections to the contribution from Z exchange are not available. Limits in the $\kappa_{tu\gamma}$–v_{tuZ} plane were derived by using a two-dimensional probability density evaluated assuming a Bayesian prior probability dis-
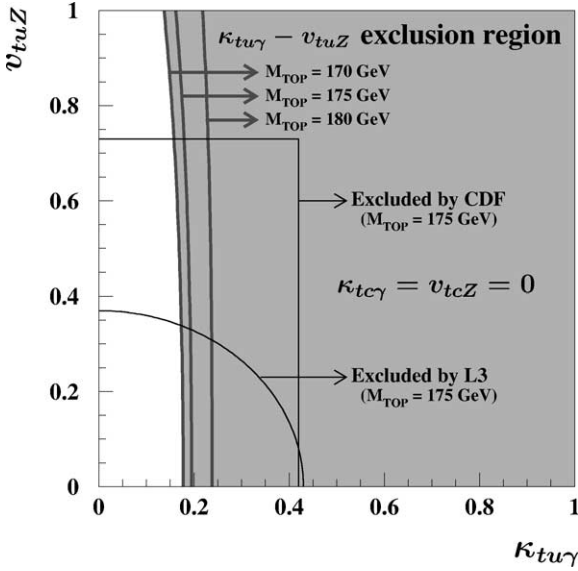
Fig. 4. Exclusion regions at 95% C.L. in the $\kappa_{tu\gamma}$–v_{tuZ} plane for three values of M_{top} (170, 175 and 180 GeV) assuming $\kappa_{tc\gamma} = v_{tcZ} = 0$. The CDF and L3 exclusion limits for $M_{top} = 175$ GeV are also shown.

tribution flat in $\kappa_{tu\gamma}$ and v_{tuZ}:

$$\rho(\kappa_{tu\gamma}, v_{tuZ}|D)$$
$$= \frac{\prod_i L_i(N^i_{obs}|\kappa_{tu\gamma}, v_{tuZ})}{\int_0^\infty d\kappa_{tu\gamma} \int_0^\infty dv_{tuZ} \prod_i L_i(N^i_{obs}|\kappa_{tu\gamma}, v_{tuZ})},$$

where $\rho(\kappa_{tu\gamma}, v_{tuZ}|D)$ is the probability density for the FCNC couplings given the set of observed data D and $L_i(N^i_{obs}|\kappa_{tu\gamma}, v_{tuZ})$ are the partial likelihoods for each channel and centre-of-mass energy evaluated as the Poissonian probabilities to observe N^i_{obs} events given the expectations of the SM background processes and the signals for single-top production. The 95% C.L. limit was found as the set of points $\rho(\kappa_{tu\gamma}, v_{tuZ}|D) = \rho_0$ such that

$$\iint_{\rho(\kappa_{tu\gamma}, v_{tuZ}|D) > \rho_0} d\kappa_{tu\gamma}\, dv_{tuZ}\, \rho(\kappa_{tu\gamma}, v_{tuZ}|D)$$
$$= 0.95.$$

Fig. 4 shows the exclusion region on the $\kappa_{tu\gamma}$–v_{tuZ} plane obtained from this search, together with those from CDF [4,50] and L3 [6], which is the most stringent limit from LEP2 [5]. It should also be noted that the Lagrangian used in the LEP analyses [5, 6,50] differs from that in Eq. (1) by a constant

multiplicative factor such that $\kappa^{LEP}_{tq\gamma} = \sqrt{2}\,\kappa^{ZEUS}_{tq\gamma}$ and $v^{LEP}_{tqZ} = \sqrt{2}\,v^{ZEUS}_{tqZ}$. In Fig. 4, the limits from CDF and L3 are plotted using the Lagrangian convention of Eq. (1). The measurements at the Tevatron and LEP have similar sensitivities to the tuV and tcV couplings, and their limits were obtained with the assumptions $\kappa_{tu\gamma} = \kappa_{tcZ}$ and $v_{tu\gamma} = v_{tcZ}$. In Fig. 4, the published CDF and L3 limits are rescaled by $\sqrt{2}$ for the purposes of comparison to the present results on $\kappa_{tu\gamma}$ and v_{tuZ} which are obtained assuming $\kappa_{tc\gamma} = v_{tcZ} = 0$. The limit-setting procedure was repeated assuming $M_{top} = 170$ and 180 GeV; the resulting exclusion regions are also shown in Fig. 4.

10. Summary

Single-top production via flavour-changing neutral current transitions has been searched for with the ZEUS detector at HERA in positron–proton and electron–proton collisions at centre-of-mass energies of 300 and 318 GeV using an integrated luminosity of 130.1 pb^{-1}. No deviation from the Standard Model prediction was found. The results were used to constrain single-top production $ep \rightarrow etX$ via the FCNC process. An upper limit on the FCNC coupling $\kappa_{tu\gamma}$ of 0.174 at 95% C.L. was obtained. This limit excludes a substantial region in $\kappa_{tu\gamma}$ not constrained by previous experiments.

M. Spira. In addition, we wish to thank E. Boos for useful discussions.

References

[1] S.L. Glashow, J. Iliopoulos, L. Maiani, Phys. Rev. D 2 (1970) 1285.

[2] H. Fritzsch, Phys. Lett. B 224 (1989) 423;
R.D. Peccei, X. Zhang, Nucl. Phys. B 337 (1990) 269;
T. Han, R.D. Peccei, X. Zhang, Nucl. Phys. B 454 (1995) 527;
G.M. Divitiis, R. Petronzio, L. Silvestrini, Nucl. Phys. B 504 (1997) 45.

[3] H. Fritzsch, D. Holtmannspötter, Phys. Lett. B 457 (1999) 186.

[4] CDF Collaboration, F. Abe, et al., Phys. Rev. Lett. 80 (1998) 2525.

[5] ALEPH Collaboration, R. Barate, et al., Phys. Lett. B 494 (2000) 33;
ALEPH Collaboration, A. Heister, et al., Phys. Lett. B 543 (2002) 173;
OPAL Collaboration, G. Abbiendi, et al., Phys. Lett. B 521 (2001) 181.

[6] L3 Collaboration, P. Achard, et al., Phys. Lett. B 549 (2002) 290.

[7] G. Schuler, Nucl. Phys. B 299 (1988) 21;
U. Baur, J.J. van der Bij, Nucl. Phys. B 304 (1988) 451;
J.J. van der Bij, G.J. van Oldenborgh, Z. Phys. C 51 (1991) 477.

[8] T. Stelzer, Z. Sullivan, S. Willenbrock, Phys. Rev. D 56 (1997) 5919;
S. Moretti, K. Odagiri, Phys. Rev. D 57 (1998) 3040.

[9] A. Belyaev, N. Kidonakis, Phys. Rev. D 65 (2002) 037501.

[10] T. Han, J.L. Hewett, Phys. Rev. D 60 (1999) 074015.

[11] A.D. Martin, et al., Eur. Phys. J. C 4 (1998) 463;
A.D. Martin, et al., Eur. Phys. J. C 14 (2000) 133.

[12] ZEUS Collaboration, in: U. Holm (Ed.), The ZEUS Detector, Status Report (unpublished), DESY, 1993, available on, http://www-zeus.desy.de/bluebook/bluebook.html.

[13] ZEUS Collaboration, M. Derrick, et al., Phys. Lett. B 293 (1992) 465.

[14] N. Harnew, et al., Nucl. Instrum. Methods A 279 (1989) 290;
B. Foster, et al., Nucl. Phys. B (Proc. Suppl.) 32 (1993) 181;
B. Foster, et al., Nucl. Instrum. Methods A 338 (1994) 254.

[15] M. Derrick, et al., Nucl. Instrum. Methods A 309 (1991) 77;
A. Andresen, et al., Nucl. Instrum. Methods A 309 (1991) 101;
A. Caldwell, et al., Nucl. Instrum. Methods A 321 (1992) 356;
A. Bernstein, et al., Nucl. Instrum. Methods A 336 (1993) 23.

[16] J. Andruszków et al., Preprint DESY-92-066, DESY, 1992;
ZEUS Collaboration, M. Derrick, et al., Z. Phys. C 63 (1994) 391;
J. Andruszków, et al., Acta Phys. Pol. B 32 (2001) 2025.

[17] W.H. Smith, K. Tokushuku, L.W. Wiggers, in: C. Verkerk, W. Wojcik (Eds.), Proc. Computing in High-Energy Physics (CHEP), Annecy, France, September 1992, CERN, Geneva, 1992, p. 222, also in preprint DESY 92-150B.

[18] R. Brun et al., GEANT3, Technical Report CERN-DD/EE/ 84-1, CERN, 1987.

[19] H.J. Kim, S. Kartik, Preprint LSUHE-145-1993, 1993.

[20] Ch. Berger, W. Wagner, Phys. Rep. 146 (1987) 1.

[21] G. Ingelman, A. Edin, J. Rathsman, Comput. Phys. Commun. 101 (1997) 108.

[22] B. Andersson, et al., Phys. Rep. 97 (1983) 31.

[23] T. Sjöstrand, Comput. Phys. Commun. 39 (1986) 347;
T. Sjöstrand, M. Bengtsson, Comput. Phys. Commun. 43 (1987) 367.

[24] A.D. Martin, R.G. Roberts, W.J. Stirling, Phys. Rev. D 50 (1994) 6734.

[25] A. Kwiatkowski, H. Spiesberger, H.-J. Möhring, Comput. Phys. Commun. 69 (1992) 155;
H. Spiesberger, An Event Generator for *ep* Interactions at HERA Including Radiative Processes (Version 4.6), 1996, available on, http://www.desy.de/~hspiesb/heracles.html.

[26] K. Charchula, G.A. Schuler, H. Spiesberger, Comput. Phys. Commun. 81 (1994) 381;
H. Spiesberger, HERACLES and DJANGOH: Event Generation for *ep* Interactions at HERA Including Radiative Processes, 1998, available on, http://www.desy.de/~hspiesb/djangoh.html.

[27] Y. Azimov, et al., Phys. Lett. B 165 (1985) 147;
G. Gustafson, Phys. Lett. B 175 (1986) 453;
G. Gustafson, U. Pettersson, Nucl. Phys. B 306 (1988) 746;
B. Andersson, et al., Z. Phys. C 43 (1989) 625.

[28] L. Lönnblad, Comput. Phys. Commun. 71 (1992) 15;
L. Lönnblad, Z. Phys. C 65 (1995) 285.

[29] H.L. Lai, et al., Eur. Phys. J. C 12 (2000) 375.

[30] T. Abe, Comput. Phys. Commun. 136 (2001) 126.

[31] U. Baur, J.A.M. Vermaseren, D. Zeppenfeld, Nucl. Phys. B 375 (1992) 3.

[32] P. Nason, R. Rückl, M. Spira, J. Phys. G 25 (1999) 1434;
M. Spira, Preprint DESY-99-060, 1999, also in: hep-ph/9905469;
K.-P.O. Diener, C. Schwanenberger, M. Spira, Eur. Phys. J. C 25 (2002) 405;
K.-P.O. Diener, C. Schwanenberger, M. Spira, hep-ex/0302040.

[33] H.L. Lai, et al., Phys. Rev. D 55 (1997) 1280.

[34] P. Aurenche, et al., Z. Phys. C 56 (1992) 589.

[35] M. Bengtsson, T. Sjöstrand, Comput. Phys. Commun. 46 (1987) 43;
T. Sjöstrand, Comput. Phys. Commun. 82 (1994) 74.

[36] M. Glück, E. Reya, A. Vogt, Phys. Rev. D 46 (1992) 1973.

[37] H1 Collaboration, C. Adloff, et al., Eur. Phys. J. C 5 (1998) 575.

[38] ZEUS Collaboration, J. Breitweg, et al., Phys. Lett. B 471 (2000) 411.

[39] ZEUS Collaboration, J. Breitweg, et al., Z. Phys. C 74 (1997) 207.

[40] ZEUS Collaboration, J. Breitweg, et al., Eur. Phys. J. C 11 (1999) 427.

[41] S. Catani, et al., Nucl. Phys. B 406 (1993) 187.

[42] S.D. Ellis, D.E. Soper, Phys. Rev. D 48 (1993) 3160.

[43] J.E. Huth, et al., in: E.L. Berger (Ed.), Research Directions for the Decade. Proceedings of Summer Study on High Energy Physics, 1990, World Scientific, 1992, p. 134, also in preprint FERMILAB-CONF-90-249-E.

[44] ZEUS Collaboration, S. Chekanov, et al., Phys. Lett. B 531 (2002) 9.

[45] H1 Collaboration, V. Andreev, et al., Preprint DESY-02-224, 2002, also in: hep-ex/0301030.

[46] H. Abramowicz, A. Caldwell, R. Sinkus, Nucl. Instrum. Methods A 365 (1995) 508;

R. Sinkus, T. Voss, Nucl. Instrum. Methods A 391 (1997) 360.

[47] ZEUS Collaboration, M. Derrick, et al., Phys. Lett. B 322 (1994) 287.

[48] ZEUS Collaboration, J. Breitweg, et al., Phys. Rev. D 63 (2001) 052002.

[49] A. Pukhov, et al., Preprint INP-MSU-98-41-542, 1999, also in: hep-ph/9908288.

[50] V.F. Obraztsov, S.R. Slabospitsky, O.P. Yushchenko, Phys. Lett. B 426 (1998) 393.